Influence of energetic disorder on electroluminescence emission in polymer:fullerene solar cells

Wei Gong,[1,2] Mark A. Faist,[2,3] Nicholas John Ekins-Daukes,[2] Zheng Xu,[1] Donal D. C. Bradley,[2]
Jenny Nelson,[2] and Thomas Kirchartz[2,*]

[1]*Key Laboratory of Luminescence and Optical Information, Ministry of Education and Institute of Optoelectronics Technology, Beijing Jiaotong University, Beijing 100044, People's Republic of China*

[2]*Department of Physics and Centre for Plastic Electronics, Imperial College London, South Kensington Campus, London SW7 2AZ, United Kingdom*

[3]*Department of Chemistry and Centre for Plastic Electronics, Imperial College London, South Kensington Campus, London SW7 2AZ, United Kingdom*

(Received 8 February 2012; published 18 July 2012)

Electroluminescence (EL) spectroscopy and imaging can be useful techniques to analyze various loss mechanisms in solar cells, but the interpretation of the results is not trivial in solar cells made from disordered materials such as organic semiconductors. In this case the interpretation of EL measurements may be affected by the presence of a tail of localized states. Here, we study several polymer:fullerene systems and show that, despite the presence of tail states, the shape of the EL spectrum is insensitive to the applied voltage. This indicates that the emission originates mainly from mobile charges in higher lying states recombining at the polymer:fullerene interface and that most charges in deeper tail states do not contribute to the EL spectrum. The consequence of our finding is that simple models of EL emission in ideal semiconductors can be applied to polymer:fullerene solar cells and can therefore be used to evaluate the potential of different material systems in terms of recombination losses and to study resistive losses using luminescence imaging.

DOI: 10.1103/PhysRevB.86.024201 PACS number(s): 84.60.Jt, 73.61.Ph, 78.60.Fi, 71.23.−k

I. INTRODUCTION

To reduce the fabrication costs of photovoltaic devices, much research on new generations of solar cells is directed towards low cost, printable thin film solar cells made from inorganic nanoparticles[1–3] or organic molecules.[4–7] Just like classical thin film solar cells such as, e.g., amorphous silicon,[8,9] these materials are generally disordered, low mobility semiconductors.[10–17] In these materials, disorder creates localized states or traps that have a strong effect on transport and likely also on nonradiative recombination.[10,18–20]

Recently, electroluminescence (EL) spectroscopy[21–24] and imaging[25,26] have been introduced as a novel (for organic semiconductors) characterization tool to study the energy levels as well as recombination and defects in polymer:fullerene solar cells. While the theoretical framework[27–30] to describe EL emission is well developed for the case of inorganic, crystalline pn-junction solar cells, the question of how applicable classical semiconductor theories are for disordered and, in this case, organic semiconductors is still under debate.[31] Simple models[32] based on the convolution of the density of states (DOS) for microcrystalline Si suggest that disorder strongly affects the description of EL emission and makes quantitative models designed for ordered semiconductors inapplicable. Whether the same applies to disordered organic solar cells has not yet been established.

In this article we focus on the study of polymer:fullerene solar cells as one class of disordered semiconductor devices and investigate to what degree the EL emission is affected by energetic disorder. A variety of experiments including charge extraction,[20,33] transient photocurrent,[10,18] and subgap quantum efficiency measurements[18,34] suggests that the most studied polymer:fullerene solar cells have a broad distribution of subgap traps or tail states. In these devices only a small high energy fraction of charge carriers dominates the transport, while the majority of the carriers are nearly immobile, i.e., trapped in lower energy states.[20] To study whether the trapped carriers or the mobile carriers dominate the radiative transitions, we study the EL as a function of applied voltage. Since the EL spectrum shifts with increasing voltage only marginally towards higher energies, we conclude that it is dominated by radiative transitions involving both mobile electrons and holes that occupy energetically higher lying states, and that emission involving localized states close to the quasi-Fermi level is suppressed due to the large spatial separation between the states at these energies. The fact that the spectral shape of the EL emission is dominated by 'free' charge carriers[35] makes it possible to use quantitative models based on the recombination of free carriers in inorganic semiconductors and has profound implications for the relation between EL and open circuit voltage[23] as well as for the interpretation of absolute EL intensities in EL imaging.[36,37]

II. THEORY

Absorption and emission between delocalized states, i.e., bands in semiconductors, are described by a convolution between the respective occupied and unoccupied states in the conduction and valence bands. The convolution[29]

$$r_a(h\upsilon) \propto \int_0^\infty M(E,h\upsilon) n_o(E) n_u(E+h\upsilon) dE = \int_0^\infty M(E,h\upsilon) \frac{N_V(E)}{1+\exp\left(\frac{E-E_{fp}}{kT}\right)} \times \frac{N_C(E+h\upsilon)}{1+\exp\left(-\frac{E+h\upsilon-E_{fn}}{kT}\right)} dE \quad (1)$$

of the concentration $n_o(E)$ of occupied states in the valence band and the concentration $n_u(E + h\upsilon)$ of unoccupied states

in the conduction band describes the absorption rate r_a, where the factor M includes the optical transition matrix element, E is the energy of electronic states, $h\upsilon$ is the photon energy, $N_{C,V}$ is the density of conduction or valence band states, E_{fn} and E_{fp} are the quasi-Fermi levels for electrons and holes, and kT is the thermal energy. Likewise, the convolution

$$r_{sp}(h\upsilon) \propto (h\upsilon)^2 \int_0^\infty M(E,h\upsilon) n_u(E) n_o(E+h\upsilon) dE$$
$$= (h\upsilon)^2 \int_0^\infty M(E,h\upsilon) \frac{N_V(E)}{1+\exp\left(-\frac{E-E_{fp}}{kT}\right)} \times \frac{N_C(E+h\upsilon)}{1+\exp\left(\frac{E+h\upsilon-E_{fn}}{kT}\right)} dE \quad (2)$$

of the concentration $n_u(E)$ of unoccupied states in the valence band and the concentration $n_o(E+h\upsilon)$ of occupied states in the conduction band describes the spontaneous emission rate r_{sp}. From Eqs. (1) and (2) it becomes clear that the shape of the DOS directly affects absorption and emission. In addition, the spectral shape is influenced by the optical transition matrix elements, which reflect the probability that a certain radiative transition occurs as a function of the energy of electron and hole and which therefore incorporates the wavefunction overlap. Although Eqs. (1) and (2) were derived for crystalline inorganic semiconductors, they can be applied to disordered semiconductors provided that the effect of state localization is incorporated into the optical transition matrix element. While there is no reason to assume that the optical transition matrix element is constant with respect to energy in either ordered or disordered semiconductors, it is often assumed to be weakly energy dependent in disordered semiconductors.[18,38] For inorganic disordered solar cell materials like amorphous silicon the transition matrix elements have been measured and hardly depend on energy for $E < 3.4$ eV,[38] but the optical matrix elements below the charge transfer (CT) state in polymer:fullerene blends have not yet been explored.

The symmetry of Eqs. (1) and (2) allowed Würfel[29] to show that absorption and emission in solar cells are intimately linked. By adding electrical transport to Würfel's theory, Rau showed that in a crystalline, asymmetric pn-junction solar cell[27,39] a simple equation connects the solar cell quantum efficiency EQE and the EL emission ϕ_{em}. This reciprocity relation

$$\phi_{em}(E) = \mathrm{EQE}(E)\phi_{bb}(E)\left[\exp\left(\frac{qV}{kT}\right) - 1\right] \quad (3)$$

implies that the shape of the EL emission spectrum ϕ_{em} depends on the product of quantum efficiency and black body spectrum ϕ_{bb} (at the temperature T of the solar cell), and the absolute intensity is controlled by the concentration of carriers and therefore by the voltage. Here and in the following, V should be interpreted as an internal voltage, which can be defined as $V = V_{ext} - JR_s$, where V_{ext} is the externally measured voltage, J is the current density, and R_s is the total series resistance including effects of the finite conductivity of the active layer as well as of the contacts (see Supplementary Material[40]). Physically, the internal voltage V in a pn-junction is defined in the context of Eq. (3) as the splitting ΔE_f of the quasi-Fermi levels (divided by the elementary charge q) in the space charge region of the pn-junction, as shown in Fig. 1(a).[28] In a thin-film solar cell, where the depletion region is not small compared to the thickness of the absorber layer, Eq. (3) does not strictly hold. However, the closest equivalent of the internal voltage would be the average splitting of the quasi-Fermi levels, as shown in Fig. 1(b). This average splitting of the quasi-Fermi level will be used in the following as a definition for internal voltage, i.e., $qV \equiv \overline{\Delta E_f}$.

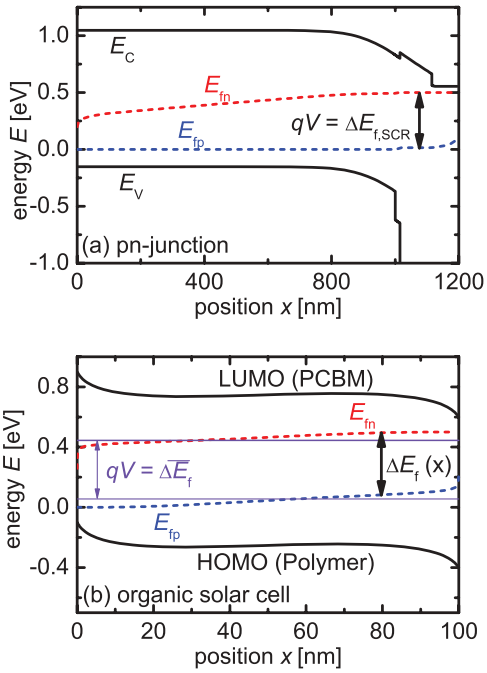

FIG. 1. (Color online) Band diagrams of a (a) pn-junction solar cell (here the example of a $Cu(In,Ga)Se_2/CdS$ solar cell) and a (b) thin organic solar cell. In case of the pn-junction solar cell, the internal voltage can be defined as the quasi-Fermi-level splitting in the space charge region, which is roughly constant. Only in the quasineutral region, the quasi-Fermi level of electrons drops drastically. In case of the organic solar cell, both quasi-Fermi levels are a function of position, and there is no region where to define a constant quasi-Fermi level. We therefore use the average quasi-Fermi-level splitting instead.

Despite the fact that Eq. (3) was neither derived for disordered semiconductors nor for devices with nonlinear recombination mechanisms like organic bulk-heterojunction solar cells,[33,41–45] it was applied to quantitatively explain the amount of observed nonradiative recombination in polymer:fullerene solar cells.[23]

III. OPTOELECTRONIC RECIPROCITY RELATIONS FOR THE CASE OF ENERGETIC DISORDER

In polymer:fullerene solar cells, an electron donor and an acceptor are blended to form the photon-absorbing layer. The absorption of the blend, however, includes a weak red-shifted component in addition to the spectrum of both blend constituents.[46–48] This feature can be attributed to an interfacial CT state that forms at the type-II heterojunction[49] between donor and acceptor molecules in organic solar cells. Electroluminescence in efficient bulk-heterojunction solar cells is—with few exceptions[50]—dominated by emission from the CT state.[24]

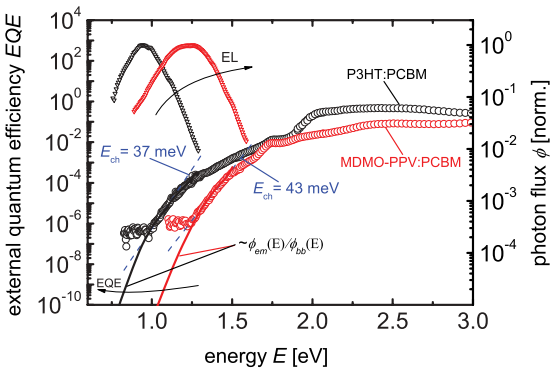

FIG. 2. (Color online) Semilogarithmic plot of experimental external quantum efficiency (EQE) (open circles), normalized electroluminescence (EL) spectrum (open triangles), and calculated EQE from EL (solid lines) as a function of energy for P3HT:PCBM (black) and MDMO-PPV:PCBM (red/dark gray) blends. The EL spectra were measured at 1250 mA/cm^2 injection current density for P3HT:PCBM and at 200 mA/cm^2 for MDMO-PPV:PCBM. The slope of the Urbach absorption tail for the two blends is also shown (blue/medium gray dashed lines).

Figure 2 shows the experimental data (EQE and EL) for two devices made from poly(3-hexylthiophene-2,5-diyl) (P3HT), poly[2-methoxy-5-(3′,7′-dimethyloctyloxy)-p-phenylene vinylene] (MDMO–PPV) and [6,6]-phenyl-C_{61} butyric acid methyl ester (PCBM). In both cases we see the absorption of the polymer at high energies followed by the distinct absorption shoulder of the PCBM at around $E = 1.75$ eV. Below the fullerene absorption shoulder, there is another kink in the spectra likely representing the CT state absorption at around 1.2 eV in case of the P3HT:PCBM blend and 1.45 eV in case of the MDMO-PPV:PCBM blend. For quantum efficiencies EQE $< 10^{-6}$, the data flattens off, indicating the limit of the sensitivity of our setup.

Using Eq. (3) and neglecting all energy-independent terms, the EQE can also be calculated from a measured EL spectrum via $\mathrm{EQE_{EL}}(E) \propto \phi_{\mathrm{em}}(E)/\phi_{\mathrm{bb}}(E)$, where the index EL indicates that the EQE is not directly measured but derived from the EL spectrum. For both blends the derived $\mathrm{EQE_{EL}}$ (solid lines) fits reasonably well to the shape of the directly measured EQE (open circles). This is due to the fact that the carrier generation in these thin absorber layers is approximately homogeneous especially for photon energies where the absorption is small. This implies that charge injection and collection effects,[28,39] which affect the validity of Eq. (3), do not depend strongly on photon energy and, thus, do not visibly affect the shape of the absorption edge of the CT state.

At low energies (absorption coefficient thickness product $\alpha d \ll 1$), the EQE is directly proportional to the absorption coefficient α if the reflectivity is roughly constant as a function of energy.[18,51] Following the approach of Street *et al.*,[18] we can thus determine the so-called Urbach energy E_{U} of the exponential absorption feature of the form

$$\mathrm{EQE}(E) \propto \alpha(E) \propto \exp\left(\frac{E}{E_{\mathrm{U}}}\right) \tag{4}$$

in the energy range between the CT state and the noise level. An exponential increase of the absorption coefficient, according to Eq. (4), is a typical feature of the absorption close to the optical band gap of disordered semiconductors and is commonly referred to as Urbach edge or Urbach's rule.[52,53] The Urbach energies E_{U} of P3HT:PCBM and MDMO-PPV:PCBM are around 37 meV and 43 meV, respectively. The value for P3HT:PCBM corresponds to the value determined by Street *et al.* for the same material,[18] and the values are similar to the typical values determined for amorphous silicon.[54] Exponential features of the low energy absorption spectrum of disordered solar cells are indicative of exponential distributions of localized states. If the conduction and valence band tails have a DOS $N_{\mathrm{CBT}}(E) \propto \exp(E/E_{\mathrm{chC}})$ and $N_{\mathrm{VBT}}(E) \propto \exp(-E/E_{\mathrm{chV}})$, respectively, it can be shown using Eq. (2) that the Urbach energy determined from absorption or quantum efficiency measurements is roughly equal to the characteristic tail slope of the broader tail [$E_{\mathrm{U}} \approx \max(E_{\mathrm{chC}}, E_{\mathrm{chV}})$]. Note that this estimation requires the transition matrix element to be energy independent. We will later discuss the implications of a nonconstant transition matrix element on this analysis.

Values around $E_{\mathrm{ch}} = 2kT$ are consistent with exponential tail slopes necessary to explain the voltage dependence of the extracted charge, as reported in Ref. 33. The measured voltage dependence of the electron and hole concentration led to the empirical relation[33]

$$\Delta n = \Delta p \propto \exp\left(\frac{qV}{mkT}\right), \tag{5}$$

where m defines the slope. As shown in Ref. 20, the slope m relates to the characteristic tail slope E_{ch} via

$$m = \frac{2E_{\mathrm{ch}}}{kT}. \tag{6}$$

For moderate doping concentrations and high forward biases, the excess electron and hole concentrations will be equal to the total carrier concentrations, and, thus, the EL emission ϕ_{em} should depend on

$$\phi_{\mathrm{em}} \propto np \propto \exp\left(\frac{2qV}{mkT}\right) = \exp\left(\frac{qV}{E_{\mathrm{ch}}}\right). \tag{7}$$

Equation (7) follows directly from Eq. (2) when using an exponential DOS and appropriate occupation probabilities, as shown by Pieters *et al.* in Ref. 32.

The voltage dependence suggested by Eq. (7) would strongly change the relation between absolute EL emission and open circuit voltage, as used by different authors to explain the open circuit voltage in polymer:fullerene solar cells[23] and different inorganic materials.[23,55,56] The quantity used to measure the absolute amount of EL emission is the external light emitting diode (LED) quantum efficiency. Unlike the solar cell quantum efficiency (EQE and $\mathrm{EQE_{EL}}$), the LED quantum efficiency Q_{LED} is a scalar quantity that is defined as the ratio of radiative recombination current density J_{rad} and the total recombination current J_{tot}, i.e.,

$$Q_{\mathrm{LED}}(V) = \frac{J_{\mathrm{rad}}(V)}{J_{\mathrm{tot}}(V)}. \tag{8}$$

The radiative recombination current is defined as the EL emission multiplied by elementary charge. Thus, no matter whether the EL emission scales with the product of free

carriers, trapped carriers [like in Eq. (7)], or a combination of both, the radiative recombination current can be written as

$$J_{\rm rad}(V) = J_{0,\rm rad}(V)\exp(V_{\rm norm}), \tag{9}$$

where $V_{\rm norm}$ is a normalized internal voltage, and $J_{0,\rm rad}$ is the radiative saturation current density. The normalized voltage will be $V_{\rm norm} = qV/kT$ in case of a crystalline semiconductor, and it would be $V_{\rm norm} = qV/E_{\rm ch}$ in case of recombination between trapped carriers in a disordered semiconductor with the same tail slope $E_{\rm ch} > kT$ for valence and conduction band tails. This assumes that the EL is determined from a direct convolution of conduction and valence band states, as described by Eq. (2), not taking into account how localized these states are, i.e., assuming constant optical transition matrix elements.

Using Eqs. (8) and (9), we can derive a relation between the loss $\Delta V_{\rm oc}$ in open circuit voltage and the logarithm of the LED quantum efficiency when going from a situation with radiative recombination only ($V_{\rm oc,rad}$) to a situation with radiative and nonradiative recombination ($V_{\rm oc}$).[27,57] However, only in the case that $V_{\rm norm} = qV/kT$ is valid will we get the relation

$$\Delta V_{\rm oc} = V_{\rm oc,rad} - V_{\rm oc} = -\frac{kT}{q}\ln(Q_{\rm LED}), \tag{10}$$

as used in all previous publications. If the radiative recombination current would follow Eq. (9) with $V_{\rm norm} = qV/E_{\rm ch}$, Eq. (10) would have to be rewritten as

$$\Delta V_{\rm oc} = V_{\rm oc,rad} - V_{\rm oc} = -\frac{E_{\rm ch}}{q}\ln(Q_{\rm LED}). \tag{11}$$

Depending on the value of the tail slope compared to kT, Eqs. (10) and (11) can predict markedly different values for $V_{\rm oc}$. Using the EQE and the EL, we can calculate the radiative open circuit voltage $V_{\rm oc,rad}$ using the method presented in Ref. 55. For P3HT:PCBM the value is $V_{\rm oc,rad} = 0.982$ V, as compared to a measured open circuit voltage $V_{\rm oc} = 0.600$ V. If we assume that the characteristic tail slope for P3HT:PCBM is 37 meV, the Urbach energy in Fig. 2, for both conduction and valence band tails and that Eq. (11) is an appropriate description of the voltage loss due to nonradiative recombination, then Eq. (10) would underestimate the loss because $kT \ll E_{\rm ch}$, leading to a predicted $V_{\rm oc} = 716$ mV (instead of the correct 600 mV). For MDMO-PPV:PCBM, the predicted $V_{\rm oc}$ would be 948 mV from Eq. (10) if Eq. (11) was correct (using $E_{\rm ch} = 40$ meV) compared to a real $V_{\rm oc} = 840$ mV. Obviously, the error of using Eq. (10) when Eq. (11) was appropriate, or vice versa is sufficiently large (>100 mV), that it would have made any proposed correlation between measured and predicted $V_{\rm oc}$ (as reported by Vandewal *et al.*[23]) impossible. The accuracy of Eq. (10) in predicting open circuit voltages when used with polymer:fullerene solar cells is thus a first indicator that the obviously present energetic disorder has a smaller effect on the voltage dependence of the EL emission than one would expect from Eqs. (2) and (11), and also that the optical matrix elements are most likely energy dependent.

IV. VOLTAGE DEPENDENCE OF THE EL PEAK POSITION

Equation (2) contains a second, easy to check, implication for the peak position of the EL as a function of voltage and injection current. Figure 3 visualizes the different effects of voltage on carrier population and emission spectra in disordered and crystalline materials. In this simple model the only difference between the crystalline and the disordered semiconductor is the shape of their DOS: the disordered semiconductor has an exponential DOS, while the crystalline semiconductor has a square-root-shaped DOS. The occupation of states, i.e., the energy-dependent concentration of electrons and holes, is calculated for simplicity by multiplying a Fermi-Dirac distribution with the respective DOS function. All transition matrix elements are assumed to be energy independent. This results in a voltage- and current-independent emission spectrum shape for the crystalline semiconductor. In contrast the peak of the carrier distribution for any exponential tail with characteristic energy $E_{\rm ch} > kT$, as shown in Fig. 3(c), will be voltage dependent.[32] Under the simplified assumption of a Fermi-Dirac occupation probability, the peak of the, e.g., electron concentration, as a function of energy can be calculated for an exponential tail from the maximum of the function

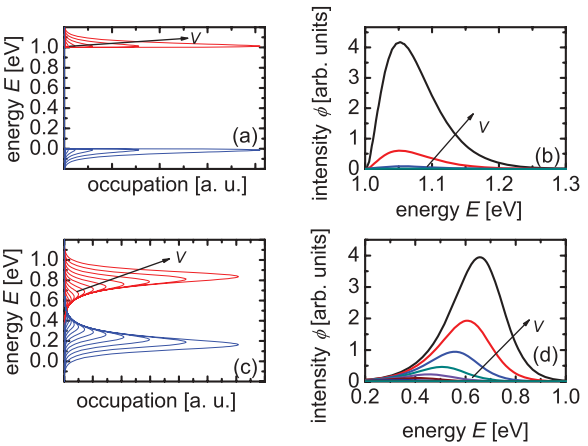

FIG. 3. (Color online) Comparison of (a) simulated carrier population in crystalline and (c) disordered materials and (b) simulated emission spectra in crystalline and (d) disordered materials for increasing applied voltage (V).

$$n(E) = N(E)f(E) = \frac{N_0\exp\left(\frac{E-E_{\rm C}}{E_{\rm ch}}\right)}{1+\exp\left(\frac{E-E_{\rm fn}}{kT}\right)}, \tag{12}$$

where N_0 is the concentration of tail states at the mobility edge $E_{\rm C}$ of the conduction band and $E_{\rm fn}$ is the quasi-Fermi level for electrons in the tail. By calculating the first derivative of Eq. (12), we calculate, for $E_{\rm ch} > kT$, the energy of the maximum of the electron concentration as

$$E_{\rm max} = E_{\rm fn} - kT\ln\left(\frac{E_{\rm ch}}{kT} - 1\right). \tag{13}$$

For $E_{\rm ch} < kT$, the distribution of carriers in the tail does not have a maximum at all, and the maximum will be at higher energies where the tail stops to increase exponentially with energy. In this case the tail can be considered nonexistent for the purpose of the study, and the behavior will be as discussed in Figs. 3(a) and 3(b) for a crystalline semiconductor. For tail slopes $E_{\rm ch} > kT$, Eq. (13) predicts that the peak of the occupation follows the quasi-Fermi level closely with a small

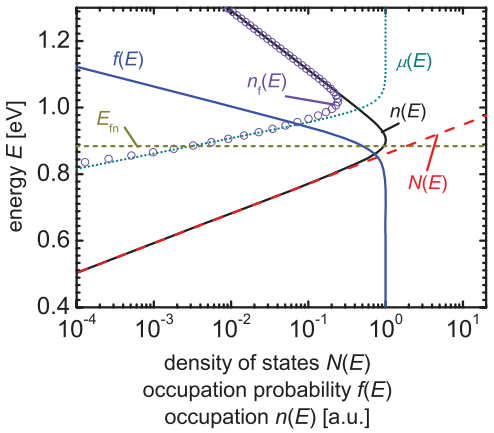

FIG. 4. (Color online) Schematic showing the relation between the exponential density of states $N(E)$, the occupation probability [Fermi-Dirac function $f(E)$], and the total carrier concentration $n(E)$. In addition, the scheme shows a hypothetical function $\mu(E)$ describing the energy-dependent mobility, which will decrease for smaller energies because of decrease in states and the increase in distance between states. From the energy-dependent carrier concentration and the energy-dependent mobility we can determine the free carrier concentration (proportional to the energy-dependent conductivity), which is above the quasi-Fermi level E_{fn} and which therefore scales with $\exp(E_{\mathrm{fn}}/kT)$.

and constant offset. The offset is only around 15 meV for $E_{\mathrm{ch}} = 40$ meV. In case both tails have characteristic energies $E_{\mathrm{ch}} > kT$, the peak of electron and hole concentration and thus the peak of their convolution will be close to the internal voltage. Figure 4 illustrates the situation with $E_{\mathrm{ch}} > kT$. The DOS $N(E)$ and the occupation function $f(E)$ control the electron concentration $n(E)$, the peak of which is close to the quasi-Fermi level for electrons E_{fn}.

Note that it is not trivial to assume that all carriers independent of energetic position and degree of localization have a common quasi-Fermi level. In standard Shockley-Read-Hall theory for disordered semiconductors,[58] the localized tail states have their own quasi-Fermi level, which is called quasi-Fermi level for trapped charge. The relation between this quasi-Fermi level and the quasi-Fermi level for mobile carriers depends on the ratio of the capture cross sections for electrons and holes. That means if the conduction band tail, for instance, traps electrons much more efficiently than it allows recombination of trapped electrons and holes, then the quasi-Fermi level for trapped charge in the conduction band will follow the quasi-Fermi level in the conduction band closely. When the conduction band tail, however, captures holes more efficiently than electrons, there will be a small offset on the order of kT. A detailed discussion of this effect is beyond the scope of this work, because the ratio of capture cross sections in organic solar cells is completely unknown so far. More detail on the theory can be found in a recent discussion of this effect in the context of thin-film silicon solar cells.[32]

To study whether the EL peak follows the population of the total carrier concentration, as predicted by Eq. (13), we would have to be able to measure the quasi-Fermi levels or at least the quasi-Fermi-level splitting $\Delta E_{\mathrm{f}} \equiv qV$ that controls the carrier population. However, the voltage we can access experimentally is only the external voltage V_{ext} that includes a drop at the series resistances in the device. Nevertheless, we know from simulations shown in the Supplementary Material[59] that the recombination current scales roughly exponentially with the average quasi-Fermi-level splitting (the internal voltage). The quantity to describe the exponential slope of current vs voltage is called the diode ideality factor, which mainly depends on the recombination mechanism and the energetic distribution of localized states in the device. The ideality factor is usually determined experimentally from the slope of the dark current/voltage curve for the range of external voltages, where the current increases exponentially and the series resistance does not dominate. However, from a conceptual point of view it is possible to extend the concept of the ideality factor beyond the range of external voltages, where it is measurable, and define it as $n_{\mathrm{id}}(V) = q/kT \times dV/d\ln(J)$. Thus, we can write the injection current as $J \sim \exp[qV/(n_{\mathrm{id}}kT)]$ with a weakly voltage-dependent value of n_{id}. Because we cannot measure n_{id} for higher voltages, we have to estimate the range of possible values. A lower ideality factor means per definition a steeper increase of current vs voltage. Thus, we expect recombination mechanisms with lower ideality factor to dominate at higher voltage, implying that the ideality factor will most likely become smaller (i.e., approach one) in the range of voltages where it is not accessible from dark current/voltage curves.

Because the injection current scales with $\exp[qV/(n_{\mathrm{id}}kT)]$, we expect the EL peak to shift by $n_{\mathrm{id}}kT/q\ \ln(10)$ per decade in injection current. For the ideality factor $n_{\mathrm{id}} = 1.41$, as measured for this particular cell for $0.2\ \mathrm{V} < V < 0.4\ \mathrm{V}$,[40] this leads to a shift of $n_{\mathrm{id}}kT/q\ \ln(10) = 84$ meV per decade in injection current. If we assume that recombination mechanisms like surface recombination,[60] which lead to lower ideality factors, become relatively more dominant at higher voltages, the ideality factor can decrease to a value of 1, which leads to $kT/q\ \ln(10) = 59$ meV.

Figure 5 shows EL spectra measured on P3HT:PCBM and MDMO-PPV:PCBM solar cells at different injection current densities between $J = 100\ \mathrm{mA\ cm^{-2}}$ to $1250\ \mathrm{mA\ cm^{-2}}$ for P3HT:PCBM and $25\ \mathrm{mA\ cm^{-2}}$ to $400\ \mathrm{mA\ cm^{-2}}$ for MDMO-PPV:PCBM. In both cases the spectra shift towards

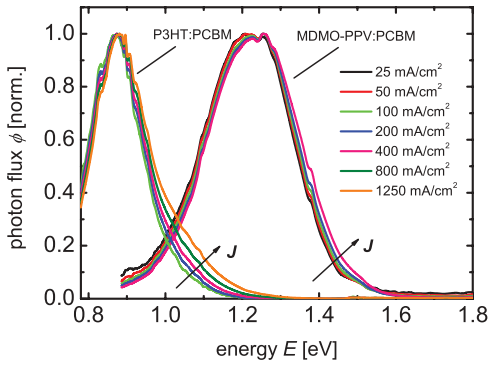

FIG. 5. (Color online) Normalized electroluminescence (EL) spectra of P3HT:PCBM and MDMO-PPV:PCBM measured at different injection current densities J. In both cases the EL shifts slightly to higher energy with increasing injection current.

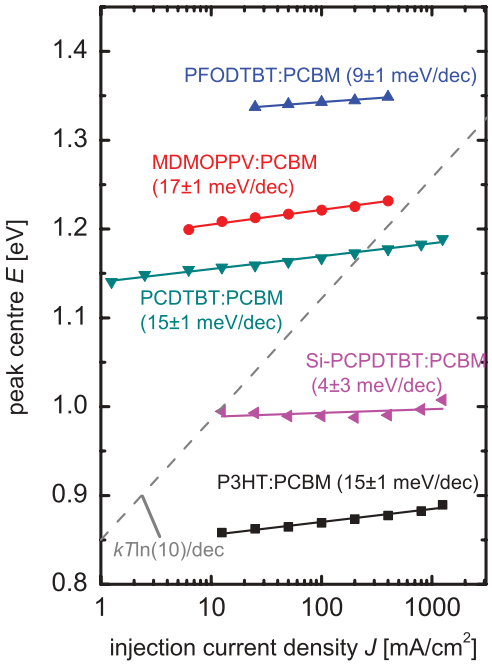

FIG. 6. (Color online) Comparison of the EL peak center shifts of different Polymer:PCBM blends. The peak center is defined as the energy about which the integral over the EL spectrum is divided into two equal halves. In both cases the peak energy shifts to higher energies with higher injection currents but with a slope that is smaller than the dashed line expected for $n_{\mathrm{id}} = 1$, electron and hole state tails with $E_{\mathrm{ch}} > kT$, and constant transition matrix elements.

higher energies for higher injection currents. The magnitude of this shift is, however, only of the order of 15 meV per decade in injection current, which is at most $1/4$ of the value expected from the shift of the convolution of electron and hole concentration in an exponential tail of states. Figure 6 shows the peak energy shift as a function of injection current for a wider variety of polymer:fullerene solar cells (see Supplementary Material[61]). In all cases we observe a blueshift of the peak with increasing injection current, but this shift is always much smaller than expected from the convolution of electron and hole densities. In the case of the Si-PCPDTBT:PCBM blend, the shift is negligible, with what little shift there is most likely attributed to temperature effects instead of a shift in carrier state occupation.

V. POSSIBLE EXPLANATIONS FOR THE SMALL INFLUENCE OF DISORDER

As explained previously, the small shift of the EL peak vs injection current cannot be explained by the application of Eq. (2) to exponential tails with slopes $E_{\mathrm{ch}} > kT$ and assuming constant optical matrix elements. Since most techniques to measure the subgap DOS are insensitive to the steeper tail, it is possible that one of the tails is so steep that it can be neglected for the purpose of this work, which implies that the concentration of carriers in this tail would follow Boltzmann approximations and would not change its peak energy with voltage. However that still leaves a shift of $kT/(2q)\ \ln(10) \approx 30$ meV to be expected, which is still larger than observed. Thus, the assumption of constant transition matrix elements cannot be correct.

If we estimate the average distance between states for a situation, as depicted in Fig. 3(c), we can make use of the typical carrier concentrations measured in P3HT:PCBM solar cells via charge extraction that lead to $10^{16}\ \mathrm{cm}^{-3} < \Delta n < 10^{17}\ \mathrm{cm}^{-3}$ in the typical measurement range up to one sun V_{oc} or in the dark for $V < 0.75$ V.[33,44] If most of the charge sits on localized states close to the quasi-Fermi level, the concentration of states will be similar to the concentration of carriers (occupation probability at the Fermi level is just $1/2$). Thus, the average distance d between two states at that energy level will be of the order $d = (\Delta n)^{-1/3}$. For example, in a blend that is mixed on the nanometer scale, a concentration $\Delta n = 10^{17}\ \mathrm{cm}^{-3}$ leads to a separation of around 22 nm, and $\Delta n = 10^{18}\ \mathrm{cm}^{-3}$ leads to 10 nm. Thus, even for carrier concentrations of $\Delta n = 10^{18}\ \mathrm{cm}^{-3}$, the distances between carriers and even between nearby states at that energy are large, and therefore the wave function overlap is limited. In a well-segregated blend the average distance between electrons and holes will be even larger.

Thus, we conclude that the convolution of electron and hole concentration is not sufficient to describe the emission, but that in addition the energy-dependent mobility influences the probability of radiative recombination events. Radiative recombination is unlikely without a preceding detrapping event that lifts one of the two carriers to a higher energy level, where it is free to move and find a partner for radiative or nonradiative recombination. Consequently, there would be no radiative transitions between the energy ranges around the two Fermi levels, but instead—as shown in Fig. 4—only higher lying states would be sufficiently mobile [i.e., free carriers $n_{\mathrm{f}}(E)$ in Fig. 4] to find a partner for recombination. Thus, the whole spectrum would be blueshifted compared to a convolution of the carrier concentrations, as given by Eq. (2). In addition, the peak shift with injection current would be reduced, as observed experimentally, since the recombining carrier populations are not close to the Fermi level. Thus, while the carrier populations would behave, as depicted in Fig. 3(c), the emission would only come from the higher lying states, thereby behaving more like Fig. 3(b) and not like Fig. 3(d).

The lack of a shift also implies that the EL emission scales roughly with $\exp(qV/kT)$, i.e., the radiative ideality factor $n_{\mathrm{id,rad}}$, which we could define as

$$n_{\mathrm{id,rad}} = \frac{q}{kT}\frac{dV}{d\ln(\phi_{\mathrm{em}})}, \tag{14}$$

will be close to 1. If only free carriers are involved in radiative recombination that are higher in energy than their quasi-Fermi level by more than $3kT$, Boltzmann approximations will be appropriate for the description of their population and

$$\phi_{\mathrm{em}} \propto n_{\mathrm{f}} p_{\mathrm{f}} \propto \exp\left(\frac{qV}{kT}\right) \tag{15}$$

will hold, where n_{f} and p_{f} are the concentrations of free electrons and holes. To say that the radiative ideality factor is unity also implies that Eq. (10) [and not Eq. (11)] will be a good approximation for the relation between open circuit voltage and absolute EL emission. The radiative ideality factor is difficult to measure directly for EL emission since—as

discussed previously—the internal voltage V can only be roughly estimated at the current densities where the EL is typically measured. Note that this discussion refers to radiative recombination only. The dominant recombination mechanism is nonradiative recombination,[23] which may occur via deep states.[62] It is likely that also nonradiative recombination requires at least one carrier to be mobile, as assumed in most recombination models involving traps.[63]

Recently, band tails have been proposed as a means to aid separation of the CT state by Street,[10] and similar arguments have been made earlier by the Janssen group.[64] The proposed mechanism assumes that the concentration of available localized states at a donor-acceptor interface is reduced compared to the bulk of the material. Thus, a CT state has a large number of options to reduce its energy by hopping to lower lying states away from the interface, while it has only a limited number of possibilities to thermalize and then recombine at the interface itself (see Fig. 11 in Ref. 10). This argument is closely connected to the observations reported here. Although most carriers do sit at lower lying localized states, there are very few of them available close to the donor/acceptor interface, making it more difficult to recombine from these low energy states.

VI. RELEVANCE FOR EL IMAGING

Understanding the mechanisms for radiative recombination at the donor/acceptor interface in disordered organic solar cells is relevant for a series of questions that go beyond the use of EL to explain the open-circuit voltage. In addition, it is relevant for deriving information about the density of available states from EL and quantum efficiency measurements as well as for the analysis of devices with EL imaging. Being already an established and popular technique in the field of inorganic photovoltaics and just an emerging technique for organic devices,[25,26] EL imaging on thin film modules can yield valuable information on resistive effects like shunts and the series resistance of the transparent conductive oxides employed.[37,65] The quantitative analysis of EL images in inorganic photovoltaics relies on the fact that the radiative recombination flux scales with $\exp(qV/kT)$, i.e., that the radiative ideality factor is one. Given the fact that the EL in polymer:fullerene blends does not shift considerably with injection current, a similar quantitative analysis, as done for inorganic thin film modules, is possible for organic modules as well.[37]

VII. RELEVANCE OF THESE FINDINGS FOR THE INTERPRETATION OF SUBGAP QUANTUM EFFICIENCY MEASUREMENTS

So far we discussed the consequences of the lack in peak shift for the interpretation of EL emission from the CT state in bulk heterojunction solar cells. However, if certain radiative transitions are suppressed because the carriers are too localized, this would also affect the inverse process of emission, namely absorption, due to detailed balance. Thus, we have to discuss whether the measurement of the Urbach energy from subgap quantum efficiency measurements, as shown in Fig. 2, is a good measure at least of the broader characteristic tail slope. To answer that question we performed simulations where we tried to reproduce the small shift in peak energy with injection current observed in P3HT:PCBM, the energetic position of the peak and the tail slope at 1.1 eV. For that we used an energy-dependent optical transition matrix element for absorption and emission, as described in the Supplementary Material.[67] The result of that simulation was that it is indeed possible to create a situation where absorption and emission are consistent with experiment using the same DOS and the same transition matrix element. However, that requires broader exponential tails, suggesting that the correct interpretation of the Urbach energy of interfacial transitions in bulk heterojunction solar cells is not straightforward and requires further study.

VIII. CONCLUSIONS

We have reported an investigation of the effect of disorder on the absorption and emission spectra of polymer:fullerene solar cells. Due to the existence of tails of localized states in disordered materials, the peak of the total electron and hole concentrations are close to the quasi-Fermi levels and will shift with voltage. However, the EL spectra of the CT state emission of polymer:fullerene solar cells show only a small blueshift with increasing voltage and injection current, indicating that the relation to the simple convolution of electron and hole concentrations is not straightforward. We propose that the energy-dependent mobility affects the probability of radiative recombination events such that only carriers with higher energies are able to recombine with each other. This implies that the radiative recombination of the CT state in polymer:fullerene blends scales with voltage most likely in a similar way as a crystalline semiconductor. This has important implications for the applicability of methods to interpret EL emission that were developed for inorganic crystalline semiconductors. In particular, all methods that require the calculation of voltages from the EL emission can be used if, as seems to be a reasonable assumption for the cells analyzed here, the radiative ideality factor can be assumed to be roughly one. Since emission is directly related to absorption, the finding that emission cannot be described by a direct convolution of two exponential tails also raises questions about the interpretation of Urbach energies from subgap quantum efficiency measurements.

ACKNOWLEDGMENTS

The authors would like to thank Louise Hirst and Markus Führer for their help with the EL setup, Jizhong Yao and Dylan Rebois for help with the determination of the spectral sensitivity of the quantum efficiency setup, and Raja Shahid Ashraf and Iain McCulloch for the synthesis of PFODTBT. The authors thank the UK Engineering and Physical Sciences Research Council (EP/F061757/1) for partial funding. W.G. acknowledges support from P.R. China's State Scholarship Fund. T.K. acknowledges support by an Imperial College Junior Research Fellowship and Bart Pieters (Jülich) for discussions on the relation between Urbach energy and characteristic energy. Z.X. thanks the National Natural Science Foundation of China under Grant No. 60978060.

APPENDIX: EXPERIMENTAL DETAILS

Poly((9,9-dioctylfiuorenyl-2,7-diyl)-alt-5,5-(40,70-di-2-thienyl-20,10,30-benzothiadiazole)) (PFODTBT) was synthesized, as described in Ref. 66. PCDTBT was purchased from 1-material and purified. P3HT was purchased from Merck, SiPCPDTBT from Konarka, MDMOPPV from Sigma-Aldrich, and $PC_{60}BM$ from Nano-C. Bulk heterojunction solar cells were prepared by cleaning patterned ITO in detergent, acetone, and isopropanol. A layer of PEDOT:PSS (Poly(3,4-ethylenedioxythiophene) poly(styrenesulfonate)) was spin coated onto the ITO substrates at 2000 rpm and annealed at 150 °C for 20 minutes. Subsequently, the active layer solution was spin coated on top [P3HT:PCBM (dissolved in chlorobenzene at 1:1wt%, 40 mg/ml), MDMO-PPV:PCBM (dissolved in chlorobenzene at 1:4wt%, 25 mg/ml), PCDTBT (dissolved in chloroform at 1:2wt%, 15 mg/ml), SiPCPDTBT (dissolved in ortho-dichlorobenzene, 1:2wt%, 40 mg/ml), PFODTBT (dissolved in ortho-dichlorobenzene, 1:4wt%, 30mg/ml)]. Vacuum-deposited aluminum (MDMOPPV:PCBM, PFODTBT:PCBM) or calcium/aluminium (P3HT:PCBM, SiPCPDTBT:PCBM, PCDTBT:PCBM) were used as cathode materials. The devices were encapsulated in a nitrogen-filled glovebox by covering the active area with a glass slide using a mixture of epoxy and hardener as glue.

External quantum efficiency was measured using monochromatic light from a monochromator (CVI DIGIKROM 240) combined with a Tungsten halogen source. The light source was chopped at 235 Hz and a lock-in amplifier (EG&G Princeton Applied Research 5210) with internal amplifier (input impedance $10^6\ \Omega$) was used to detect the photocurrent. Long pass filters at 610, 715, 780, 850, and 1000 nm were used to filter out the scattered light from the monochromator. The spectrum was calculated using calibrated photodiodes (a silicon photodiode between 350 − 1100 nm and a germanium photodiode above 1100 nm). The spectral sensitivity of the setup was measured by measuring the quantum efficiency of a GaAs-based solar cell with much steeper absorption edge than the disordered materials discussed here. The absorption edge of the GaAs-based cell had an Urbach energy of 7 meV, which is much smaller than the Urbach energies reported here.

Electroluminescence was measured at current densities of $1.25-1250\ mA/cm^2$ using a Princeton Instruments Acton SP 2500 monochromator combined with a liquid nitrogen-cooled InGaAs photodiode array (Acton OMAV:1024). Spectral intensity was corrected with the spectrum from a calibrated halogen lamp.

The peaks of the EL spectra were determined by integrating over the normalized peak using the energies as integration boundaries where the EL spectrum was at 30% of the peak to avoid any influence from noise and temperature effects. The peak was chosen to be the energy that divides the integral in two equal halves.

*Corresponding author: t.kirchartz@imperial.ac.uk

[1] E. H. Sargent, Nature Photonics **3**, 325 (2009).
[2] J. M. Luther, M. Law, M. C. Beard, Q. Song, M. O. Reese, R. J. Ellingson, and A. J. Nozik, Nano Lett. **8**, 3488 (2008).
[3] S. A. McDonald, G. Konstantatos, S. G. Zhang, P. W. Cyr, E. J. D. Klem, L. Levina, and E. H. Sargent, Nat. Mater. **4**, 138 (2005).
[4] F. C. Krebs, Solar Energy Materials and Solar Cells **93**, 1636 (2009).
[5] C. J. Brabec and J. R. Durrant, MRS Bull. **33**, 670 (2008).
[6] M. M. Voigt, R. C. I. MacKenzie, C. P. Yau, P. Atienzar, J. Dane, P. E. Keivanidis, D. D. C. Bradley, and J. Nelson, Solar Energy Materials and Solar Cells **95**, 731 (2011).
[7] X. Wang, T. Ishwara, W. Gong, M. Campoy-Quiles, J. Nelson, and D. D. C. Bradley, Adv. Funct. Mater. **22**, 1454 (2012).
[8] T. Tiedje, Appl. Phys. Lett. **40**, 627 (1982).
[9] T. Tiedje, J. M. Cebulka, D. L. Morel, and B. Abeles, Phys. Rev. Lett. **46**, 1425 (1981).
[10] R. A. Street, Phys. Rev. B **84**, 075208 (2011).
[11] J. Nelson, Phys. Rev. B **67**, 155209 (2003).
[12] M. Tachiya and K. Seki, Phys. Rev. B **82**, 085201 (2010).
[13] G. Garcia-Belmonte, P. P. Boix, J. Bisquert, M. Lenes, H. J. Bolink, A. La Rosa, S. Filippone, and N. Martin, J. Phys. Chem. Lett. **1**, 2566 (2010).
[14] G. Garcia-Belmonte and J. Bisquert, Appl. Phys. Lett. **96**, 113301 (2010).
[15] S. M. Tuladhar, D. Poplavskyy, S. A. Choulis, J. R. Durrant, D. D. C. Bradley, and J. Nelson, Adv. Funct. Mater. **15**, 1171 (2005).
[16] Y. Kim, S. Cook, S. M. Tuladhar, S. A. Choulis, J. Nelson, J. R. Durrant, D. D. C. Bradley, M. Giles, I. McCulloch, C. S. Ha, and M. Ree, Nat. Mater. **5**, 197 (2006).
[17] S. A. Choulis, J. Nelson, Y. Kim, D. Poplavskyy, T. Kreouzis, J. R. Durrant, and D. D. C. Bradley, Appl. Phys. Lett. **83**, 3812 (2003).
[18] R. A. Street, K. W. Song, J. E. Northrup, and S. Cowan, Phys. Rev. B **83**, 165207 (2011).
[19] R. C. I. MacKenzie, T. Kirchartz, G. F. A. Dibb, and J. Nelson, J. Phys. Chem. C **115**, 9806 (2011).
[20] T. Kirchartz, B. E. Pieters, J. Kirkpatrick, U. Rau, and J. Nelson, Phys. Rev. B **83**, 115209 (2011).
[21] K. Tvingstedt, K. Vandewal, F. L. Zhang, and O. Inganas, J. Phys. Chem. C **114**, 21824 (2010).
[22] K. Vandewal, K. Tvingstedt, J. V. Manca, and O. Inganas, IEEE J. Sel. Top. Quantum Electron. **16**, 1676 (2010).
[23] K. Vandewal, K. Tvingstedt, A. Gadisa, O. Inganas, and J. V. Manca, Nat. Mater. **8**, 904 (2009).
[24] K. Tvingstedt, K. Vandewal, A. Gadisa, F. L. Zhang, J. Manca, and O. Inganas, J. Am. Chem. Soc. **131**, 11819 (2009).
[25] U. Hoyer, M. Wagner, T. Swonke, J. Bachmann, R. Auer, A. Osvet, and C. J. Brabec, Appl. Phys. Lett. **97**, 233303 (2010).
[26] M. Seeland, R. Rosch, and H. Hoppe, J. Appl. Phys. **109**, 064513 (2011).
[27] U. Rau, Phys. Rev. B **76**, 085303 (2007).
[28] T. Kirchartz and U. Rau, Phys Status Solidi A **205**, 2737 (2008).
[29] P. Würfel, J. Phys. C **15**, 3967 (1982).

[30]P. Würfel, T. Trupke, T. Puzzer, E. Schaffer, W. Warta, and S. W. Glunz, J. Appl. Phys. **101**, 123110 (2007).
[31]M. C. Scharber, C. Lungenschmied, H.-J. Egelhaaf, G. Matt, M. Bednorz, T. Fromherz, J. Gao, D. Jarzab, and M. A. Loi, Energ. Environ. Sci. **4**, 5077 (2011).
[32]B. E. Pieters, T. Kirchartz, T. Merdzhanova, and R. Carius, Solar Energy Materials and Solar Cells **94**, 1851 (2010).
[33]C. G. Shuttle, A. Maurano, R. Hamilton, B. O'Regan, J. C. de Mello, and J. R. Durrant, Appl. Phys. Lett. **93**, 183501 (2008).
[34]M. Presselt, M. Barenklau, R. Rosch, W. J. D. Beenken, E. Runge, S. Shokhovets, H. Hoppe, and G. Gobsch, Appl. Phys. Lett. **97**, 253302 (2010).
[35]In this context we refer to free carriers in the sense of a multiple trapping-type model, where the free and trapped carriers are separated by a demarcation energy, called the mobility edge. Carriers in higher energy levels are assumed mobile, and carriers with lower energy are assumed to be completely localized.
[36]U. Hoyer, L. Pinna, T. Swonke, R. Auer, C. J. Brabec, T. Stubhan, and N. Li, Advanced Energy Materials **1**, 1097 (2011).
[37]M. Seeland, R. Rosch, and H. Hoppe, J. Appl. Phys. **111**, 024505 (2012).
[38]W. B. Jackson, S. M. Kelso, C. C. Tsai, J. W. Allen, and S. J. Oh, Phys. Rev. B **31**, 5187 (1985).
[39]T. Kirchartz, J. Mattheis, and U. Rau, Phys. Rev. B **78**, 235320 (2008).
[40]See Supplemental Material Figure S1 at http://link.aps.org/supplemental/10.1103/PhysRevB.86.024201 for a definition of internal voltage.
[41]C. G. Shuttle, B. O'Regan, A. M. Ballantyne, J. Nelson, D. D. C. Bradley, J. de Mello, and J. R. Durrant, Appl. Phys. Lett. **92**, 093311 (2008).
[42]C. G. Shuttle, B. O'Regan, A. M. Ballantyne, J. Nelson, D. D. C. Bradley, and J. R. Durrant, Phys. Rev. B **78**, 113201 (2008).
[43]C. G. Shuttle, R. Hamilton, B. C. O'Regan, J. Nelson, and J. R. Durrant, Proc. Natl. Acad. Sci. USA **107**, 16448 (2010).
[44]A. Maurano, R. Hamilton, C. G. Shuttle, A. M. Ballantyne, J. Nelson, B. O'Regan, W. M. Zhang, I. McCulloch, H. Azimi, M. Morana, C. J. Brabec, and J. R. Durrant, Adv. Mater. **22**, 4987 (2010).
[45]D. Credgington, R. Hamilton, P. Atienzar, J. Nelson, and J. R. Durrant, Adv. Funct. Mater. **21**, 2744 (2011).
[46]L. Goris, K. Haenen, M. Nesladek, P. Wagner, D. Vanderzande, L. De Schepper, J. D'Haen, L. Lutsen, and J. V. Manca, J. Mater. Sci. **40**, 1413 (2005).
[47]L. Goris, A. Poruba, L. Hod'ákova, M. Vaněček, K. Haenen, M. Nesládek, P. Wagner, D. Vanderzande, L. De Schepper, and J. V. Manca, Appl. Phys. Lett. **88**, 052113 (2006).
[48]J. J. Benson-Smith, L. Goris, K. Vandewal, K. Haenen, J. V. Manca, D. Vanderzande, D. D. C. Bradley, and J. Nelson, Adv. Funct. Mater. **17**, 451 (2007).
[49]Type II here means that the band offsets for conduction and valence band have the same sign, meaning that one of the materials is energetically more favorable for electrons and one for holes.
[50]E. G. Wang, Z. F. Ma, Z. Zhang, K. Vandewal, P. Henriksson, O. Inganas, F. L. Zhang, and M. R. Andersson, J. Am. Chem. Soc. **133**, 14244 (2011).
[51]J. Lee, K. Vandewal, S. R. Yost, M. E. Bahlke, L. Goris, M. A. Baldo, J. V. Manca, and T. Van Voorhis, J. Am. Chem. Soc. **132**, 11878 (2010).
[52]F. Urbach, Phys. Rev. **92**, 1324 (1953).
[53]N. F. Mott and E. A. Davis, *Electronic Processes in Non-Crystalline Materials* (Clarendon Press, Oxford, 1979), p. 275.
[54]J. J. Liang, E. A. Schiff, S. Guha, B. J. Yan, and J. Yang, Appl. Phys. Lett. **88**, 063512 (2006).
[55]T. Kirchartz and U. Rau, J. Appl. Phys. **102**, 104510 (2007).
[56]T. Kirchartz, A. Helbig, W. Reetz, M. Reuter, J. H. Werner, and U. Rau, Progress in Photovoltaics **17**, 394 (2009).
[57]T. Kirchartz, U. Rau, M. Kurth, J. Mattheis, and J. H. Werner, Thin Solid Films **515**, 6238 (2007).
[58]J. G. Simmons and G. W. Taylor, Phys. Rev. B **4**, 502 (1971).
[59]See Supplemental Material Figure S2 at http://link.aps.org/supplemental/10.1103/PhysRevB.86.024201 for a drift-diffusion simulation showing that the recombination current is exponential with the average quasi-Fermi-level splitting.
[60]T. Kirchartz, B. E. Pieters, K. Taretto, and U. Rau, Phys. Rev. B **80**, 035334 (2009).
[61]See Supplemental Material Figure S3 at http://link.aps.org/supplemental/10.1103/PhysRevB.86.024201 for injection current-dependent EL spectra of PFODTBT:PCBM, PCDTBT:PCBM, and Si-PCPDTBT:PCBM.
[62]R. A. Street, M. Schoendorf, A. Roy, and J. H. Lee, Phys. Rev. B **81**, 205307 (2010).
[63]B. E. Pieters, K. Decock, M. Burgelman, R. Stangl, and T. Kirchartz, in *Advanced Characterization Techniques for Thin Film Solar Cells*, (Wiley-VCH, Verlag, GmbH & Co., KGaA, 2011), p. 501.
[64]T. Offermans, S. C. J. Meskers, and R. A. J. Janssen, J. Chem. Phys. **119**, 10924 (2003).
[65]A. Helbig, T. Kirchartz, R. Schaeffler, J. H. Werner, and U. Rau, Solar Energy Materials and Solar Cells **94**, 979 (2010).
[66]M. A. Faist, T. Kirchartz, W. Gong, R. S. Ashraf, I. McCulloch, J. C. de Mello, N. J. Ekins-Daukes, D. D. C. Bradley, and J. Nelson, J. Am. Chem. Soc. **134**, 685 (2012).
[67]See Supplemental Material section I at http://link.aps.org/supplemental/10.1103/PhysRevB.86.024201 for, the details of the simulations done to model quantum efficiency and EL peak shift.